

## Supplementary information

### Towards Molecular Dynamics Simulation of Membrane-Targeting Photosensitizing Antivirals

Irina S. Panina<sup>1,2</sup>, Yulia S. Vlasova<sup>1,3</sup>, Yulia S. Panina<sup>4</sup>, Maxim S. Krasilnikov<sup>1</sup>, Vera A. Alferova<sup>1</sup>, Vladimir A. Korshun<sup>1</sup>, Anton O. Chugunov<sup>1,2,3\*</sup>

<sup>1</sup> Shemyakin-Ovchinnikov Institute of Bioorganic Chemistry, Moscow 117997, Russia.

<sup>2</sup> Scientific Research Institute for Systems Biology and Medicine, Moscow 117246, Russia.

<sup>3</sup> Moscow Center for Advanced Studies, Moscow 123592, Russia.

<sup>4</sup> Vavilov Institute of General Genetics, Moscow 119991, Russia

\* Corresponding author: [batch2k@yandex.ru](mailto:batch2k@yandex.ru)

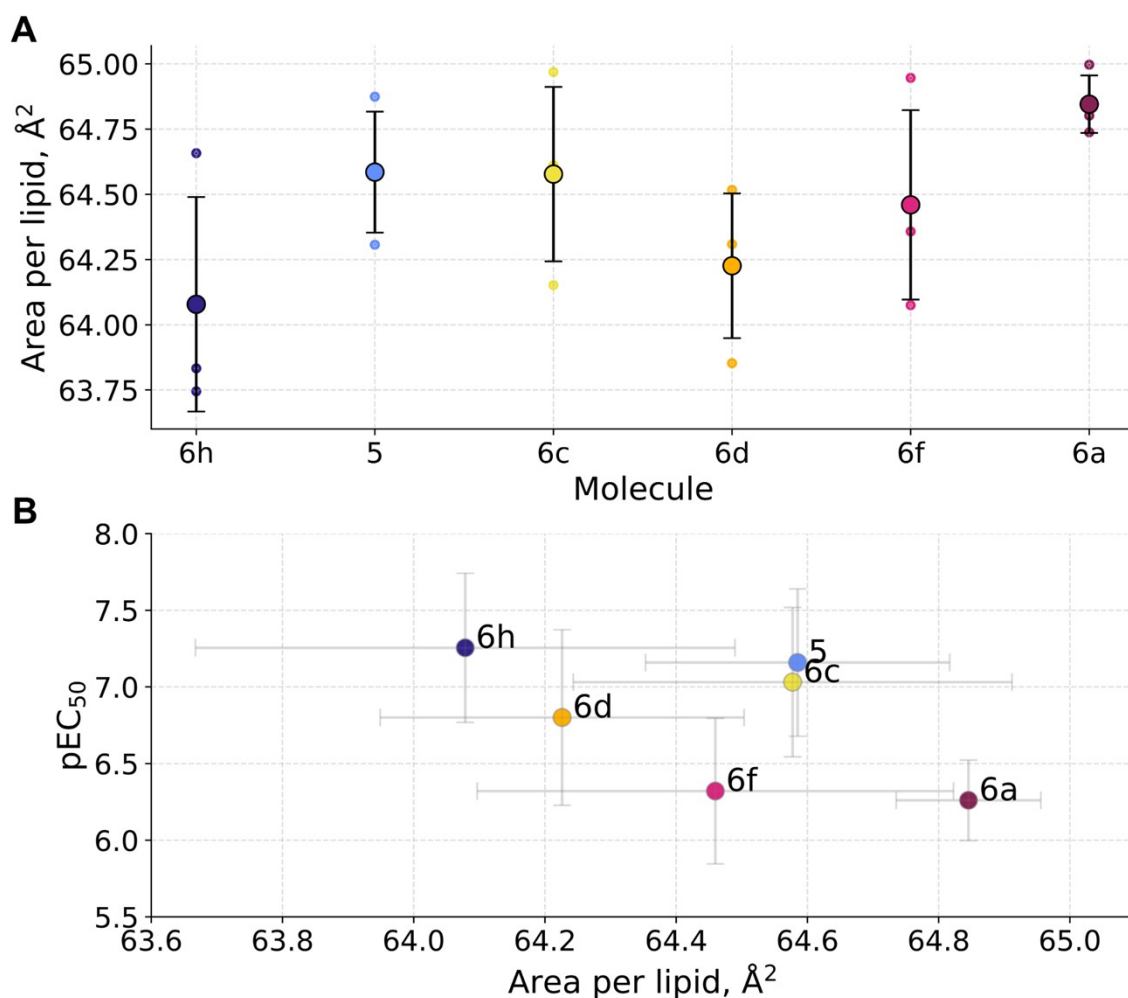


**Figure S1. Effect of perylene derivative insertion on bilayer structural properties.** The area per lipid (APL) (A) and its correlation with antiviral activity (B). The APL values represent averages over three independent MD simulations (*large circles*), with individual simulation means depicted as *smaller colored circles*. Note that the observed decrease in APL for the most active compounds generally remains within the margin of error.

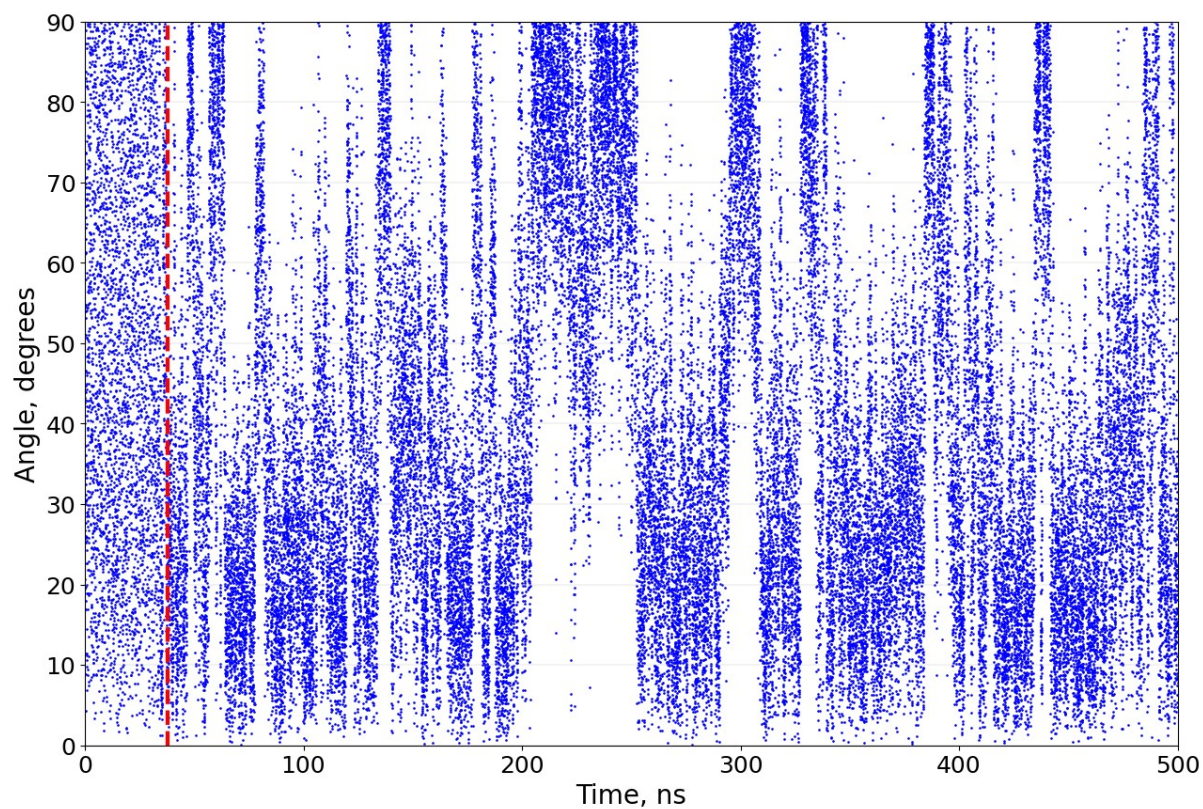


**Figure S2. Orientation of perylene–uracil rings during MD** (example for compound **6a**). The plot measures dihedral angle between perylene and uracil planar groups vs. simulation time. The *red dashed line* at 38 ns marks the moment of the compound insertion into the bilayer.

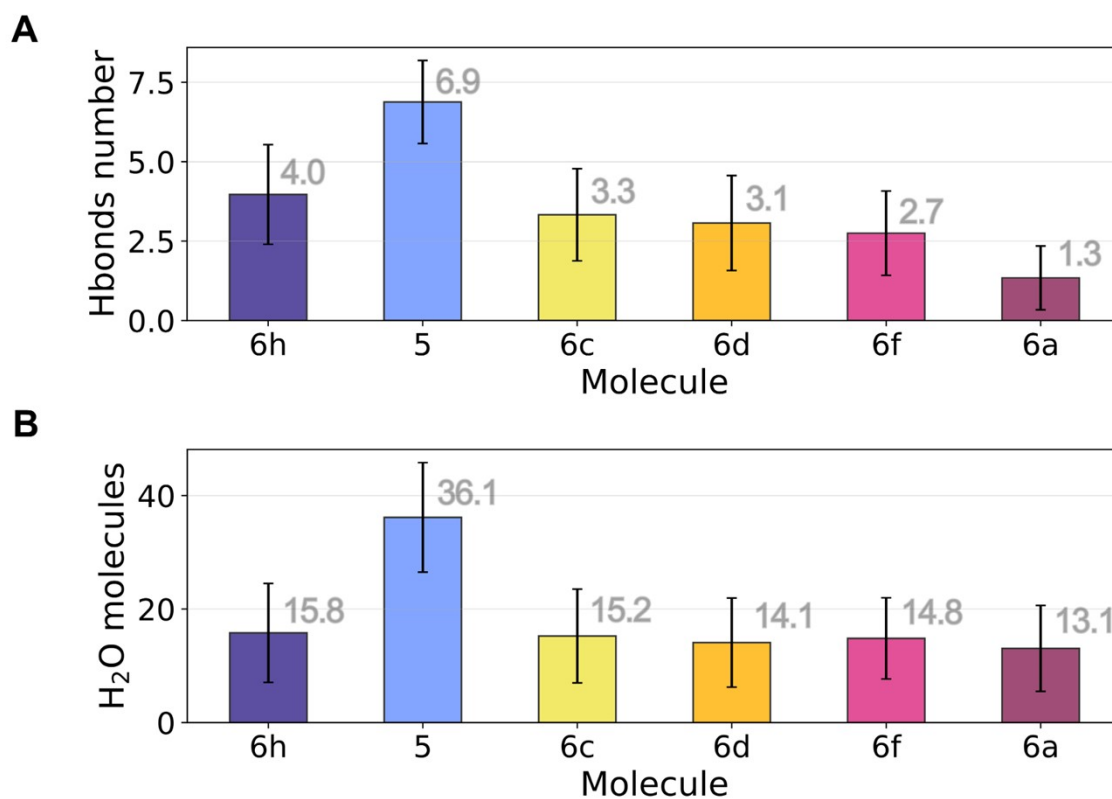
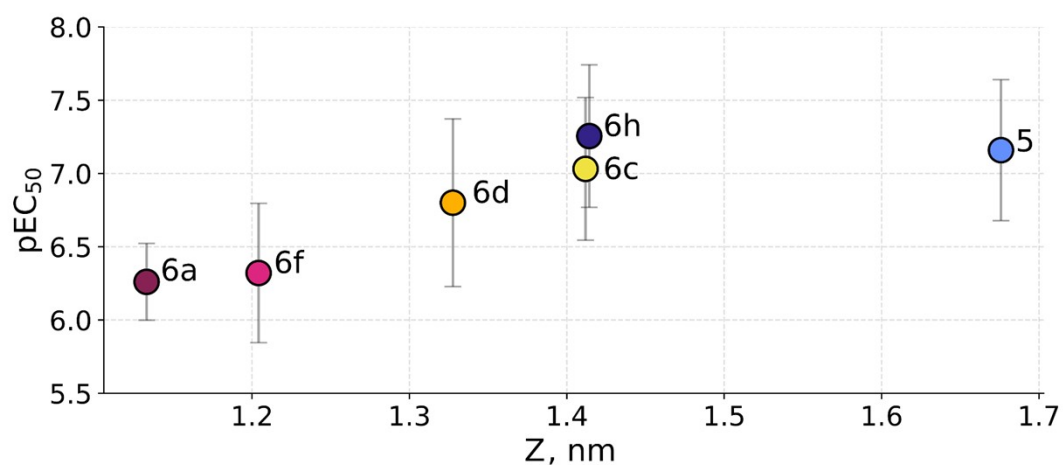


**Figure S3. Solvent exposure of membrane-embedded perylene derivatives.** **A.** The average number of hydrogen bonds formed between the compounds and water, calculated over 3 independent MD runs. **B.** Surface accessibility of the perylene group, quantified as the number of water molecules within 0.35 nm. Compounds with higher antiviral activity show slightly increased solvent accessibility.

**A:** Antiviral activity vs Uracil depth



**B:** Antiviral activity vs Perylene depth

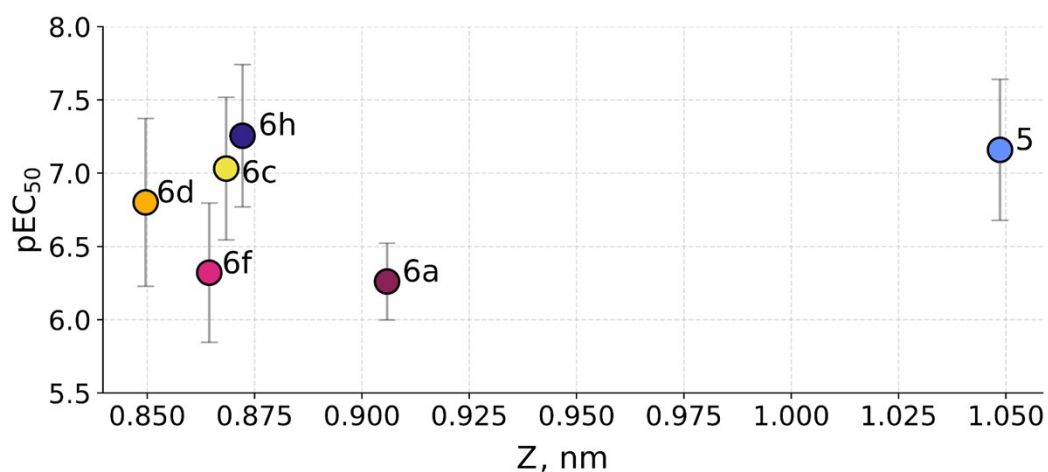


**Figure S4. The connection between antiviral activity and average membrane positions of uracil (A) and perylene (B) moieties in MD.** The depth of the perylene group showed no correlation with activity (see also Fig. 2B in the main text). In contrast, among the uncharged homologous compounds **6**, molecules with a higher uracil position tended towards increased antiviral efficacy (see also Fig. 2A).

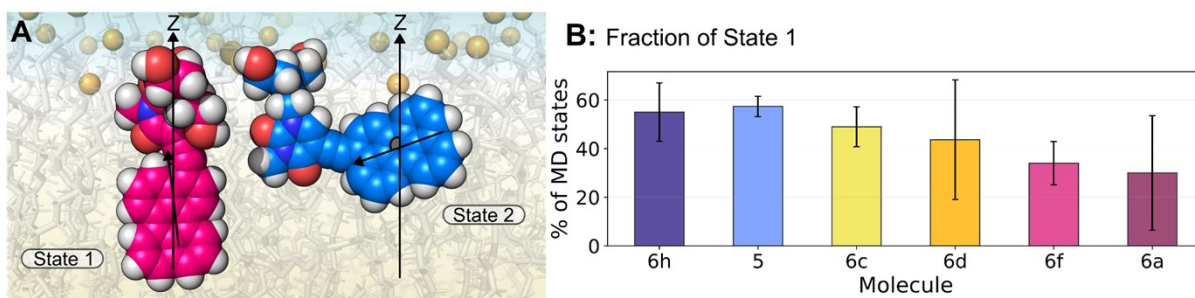


**Figure S5. Preferential orientations of perylene derivatives within the lipid bilayer during MD simulations.** **A.** Two characteristic binding orientations, defined by a molecular tilt angle threshold of  $50^\circ$ : state 1 (*magenta*,  $<50^\circ$ ) and state 2 (*blue*,  $>50^\circ$ ), shown for **6h** (the same is true for other compounds). **B.** MD lifetime of state 1, averaged over three replicas, correlates with compound activity, with more active compounds exhibiting longer state 1 lifetimes.

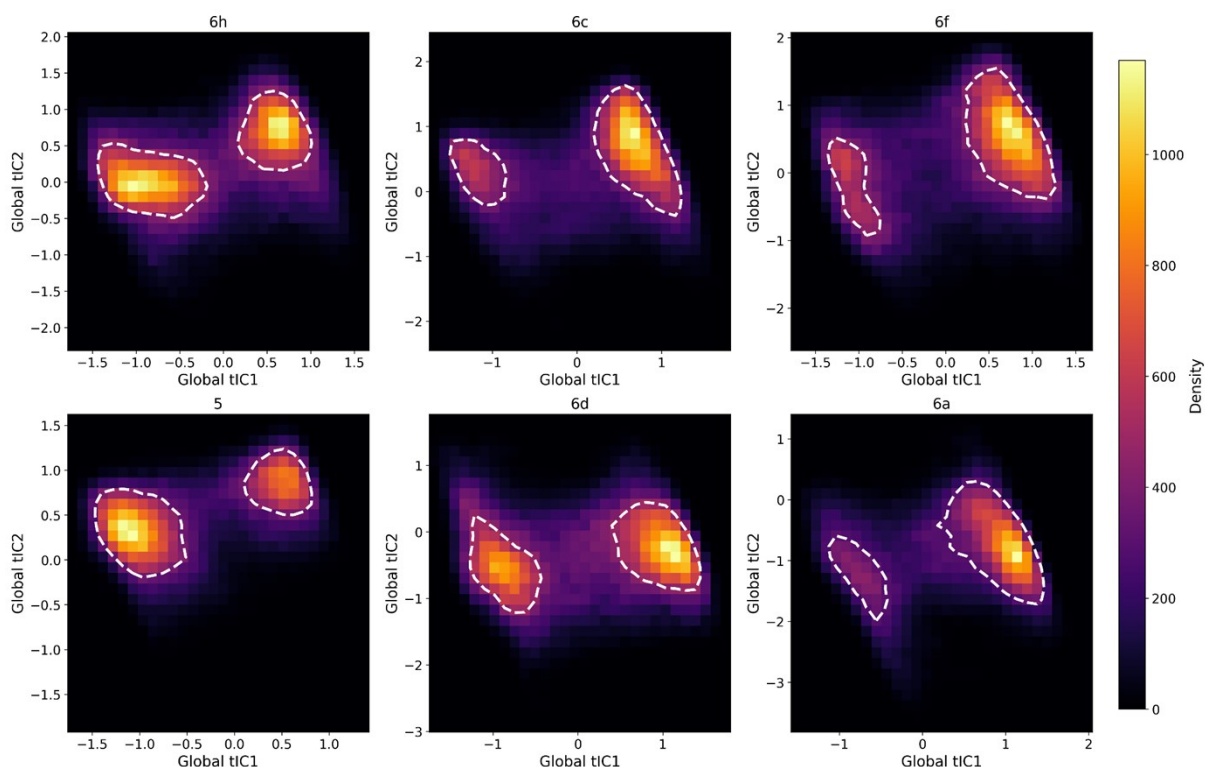


**Figure S6. TICA projection landscapes for six perylene derivatives in MD.** Two-dimensional energy-like landscapes were constructed from MD trajectories using tICA with a lag time of 200 ps. Each heatmap represents the probability density distribution of molecular conformations projected on the first two slowest tICA coordinates (tIC1 and tIC2), averaged over three MD replicas for each compound. The *white dashed contours* indicate the 85<sup>th</sup> percentile density threshold, enclosing the most populated conformational states. The color gradient represents increasing conformational density, with the scale normalized across all systems to enable direct comparison. TICA parameterization was conducted on the whole dataset consisting of 18 MD trajectories, providing uniform and directly comparable coordinates:  $\text{global tIC1} = 0.395 \times \text{vecvec\_ang} + (-0.390) \times \text{Z\_tail} + (-0.271) \times \text{vec\_ang} + 0.241 \times \text{vecH\_ang} + 0.235 \times \text{plane\_ang} + (-0.050) \times \text{sasa} + (-0.044) \times \text{planeU\_ang} + 0.042 \times \text{Z\_per}$ ; and  $\text{global tIC2} = 0.813 \times \text{Z\_tail} + 0.525 \times \text{vec\_ang} + (-0.320) \times \text{plane\_ang} + 0.151 \times \text{planeU\_ang} + (-0.135) \times \text{Z\_per} + (-0.064) \times \text{vecvec\_ang} + (-0.064) \times \text{vecH\_ang} + 0.023 \times \text{sasa}$ . Here, features are ordered according to their significance; the meaning is provided in *Methods*.

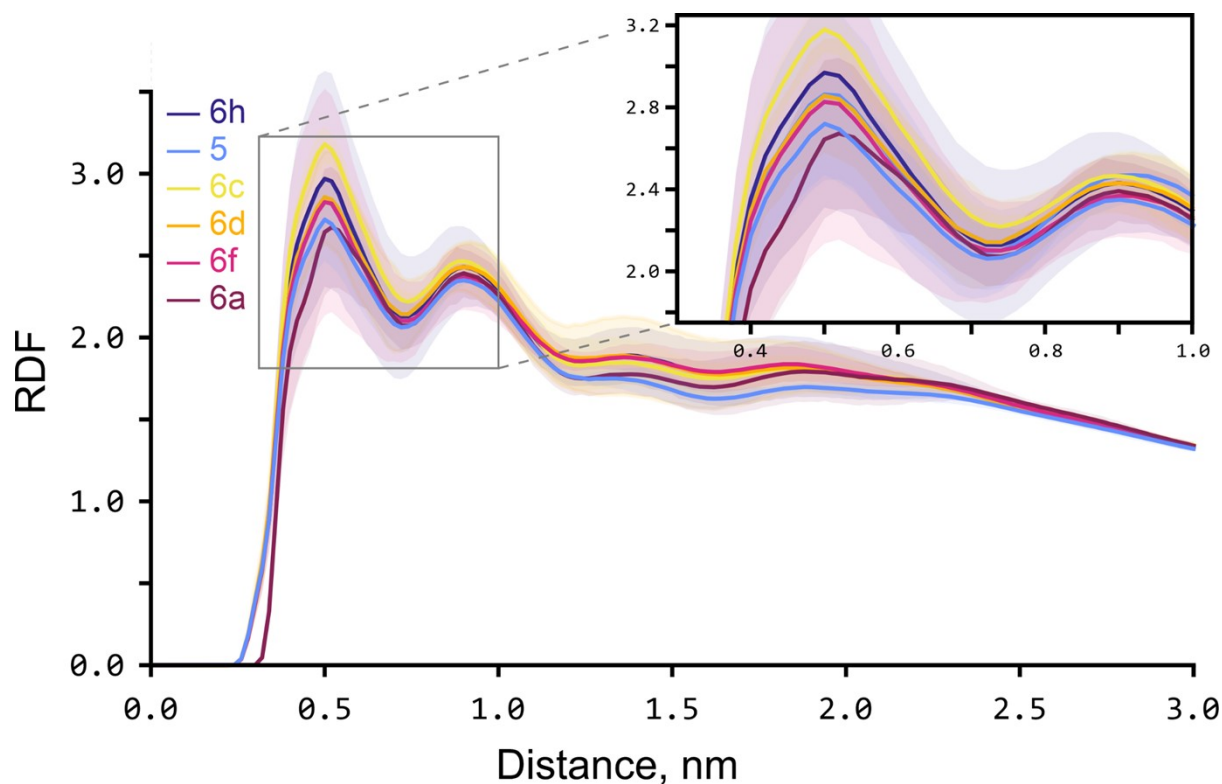


**Figure S7. Radial distribution functions (RDFs) of carbon atoms in POPC molecules forming the double bond, relative to the perylene core.** The *solid lines* represent the RDF for each individual compound, averaged over three MD replicas (*shaded area* is standard deviation). The *inset* shows a close-up view of the first peak, which suggests a trend, although not clearly defined, that there may be more double bonds near the perylene for more active molecules that belong to homologous series **6** with an uncharged R-group, except for **5** possessing a charged carboxyl group.

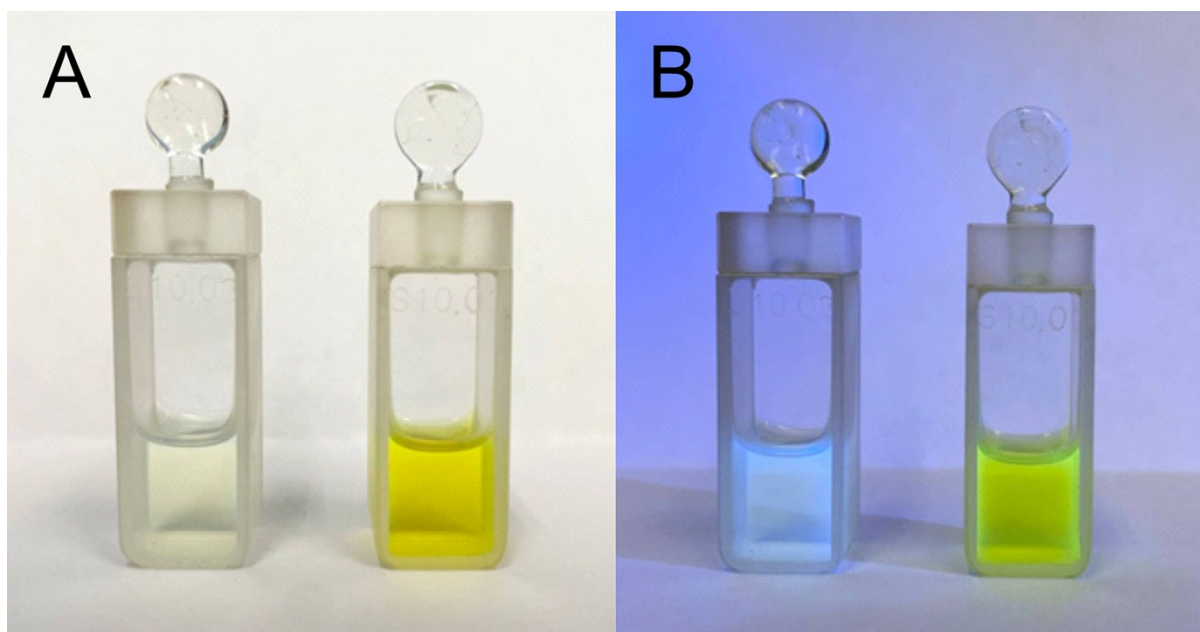


**Figure S8.** Solutions (30  $\mu\text{M}$ ) of perylene (*left*) and compound **6a** (*right*) in 96% aq. ethanol under daylight (**A**) and 356 nm UV lamp illumination (**B**).

**Video S1. Molecule 6f insertion into the POPC bilayer.** Fragment of an MD trajectory (40–60 ns) illustrating the embedding of the compound from solvent phase into the lipid bilayer. Pymol function *smooth* was applied to the trajectory for clarity.

**Video S2. Flip-flop of 6d molecule during one of MD trajectories.** Fragment of an MD trajectory (20–70 ns) illustrating the flopping from the upper leaflet of the lipid bilayer to the lower one. Pymol function *smooth* was applied to the trajectory for clarity.